OH, HO_2, and Ozone Gaseous Diffusion Coefficients

Andrey V. Ivanov,* Sofia Trakhtenberg,† Allan K. Bertram,‡ Yulii M. Gershenzon,§ and Mario J. Molina

Department of Chemistry and Biochemistry, University of California-San Diego, La Jolla, California 92039

Received: October 5, 2006; In Final Form: January 5, 2007

The diffusion of OH, HO_2, and O_3 in He, and of OH in air, has been investigated using a coated-wall flow tube reactor coupled to a chemical ionization mass spectrometry. The diffusion coefficients were determined from measurements of the loss of the reactive species to the flow tube wall as a function of pressure. On the basis of the experimental results, $D_{OH-He} = 662 \pm 33$ Torr cm^2 s^{-1}, $D_{OH-air} = 165 \pm 20$ Torr cm^2 s^{-1}, $D_{HO_2-He} = 430 \pm 30$ Torr cm^2 s^{-1}, and $D_{O_3-He} = 410 \pm 25$ Torr cm^2 s^{-1} at 296 K. We show that the measured values for OH and HO_2 are in better agreement with measured values of their polar analogues (H_2O and H_2O_2) compared with measured values of their nonpolar analogues (O and O_2). The measured value for OH in air is 25% smaller than that for O (the nonpolar analogue). The difference between the measured value for HO_2 and O_2 (the nonpolar analogue) in air is expected to be even larger. Also we show that calculations of the diffusion coefficients based on Lennard−Jones potentials are in excellent agreement with the measurements. This gives further confidence that these calculations can be used to estimate accurate diffusion coefficients for conditions where laboratory data currently do not exist.

Introduction

Research over the past 20 years has shown that reactions between trace gas-phase species and aerosol particles and cloud droplets (termed heterogeneous chemistry) play an important role in the atmosphere. OH, HO_2, and O_3 are examples of trace gas-phase species that can undergo important heterogeneous reactions in the atmosphere. For example, it has recently been shown that OH radicals can oxidize organic particles, and this reaction may be an important loss process of organic material in the atmosphere.[1,2] Also, reactions of both OH and HO_2 (also called HO_x) with cloud droplets play an important role in cloud chemistry.[3−8] Other heterogeneous reactions that are thought to be important include HO_x uptake on sea salt particles[9−11] and cirrus clouds[12−16] and O_3 uptake on fresh soot particles. In the later case, O_3 is thought to oxidize the soot particles and hence change the hygroscopic properties of soot particles, which may affect the soot lifetime in the atmosphere under certain conditions.[17]

The loss of gas-phase species to atmospheric particles and cloud droplets can be controlled by both diffusion to the particle/droplet surface or the reaction rate at the particle/droplet surface. The overall rate constant for heterogeneous loss, k_{obs}, to a particle/droplet surface can be described by the following equation (which is based on rule of the additivity of kinetic resistances[18]):

$$\frac{1}{k_{obs}} = \frac{1}{k_{het}} + \frac{1}{k_{dif}} \tag{1}$$

where k_{het} is the kinetic rate constant of heterogeneous loss which depends on an uptake coefficient and the mean thermal velocity and k_{dif} is the diffusion rate constant to the particle/droplet surface. k_{dif} can be described by the following equation:[5]

$$k_{dif} = \frac{3D_g}{r_p^2}V = 4\pi r_p D_g n \tag{2}$$

where D_g is the gas-phase diffusion coefficient, V is the particle volume, and n is the aerosol number density. Combining eq 1 and 2 gives the following equation:

$$\frac{1}{k_{obs}} = \frac{1}{k_{het}} + \frac{1}{4\pi r_p D_g n} \tag{3}$$

Equation 3 shows that in order to predict the observed first-order loss rated of gas-phase species, such as OH, HO_2, and O_3, to atmospheric particles and droplets, knowledge of the diffusion coefficient is required.

In laboratory studies, knowledge of diffusion coefficients is also required to accurately determine reactive uptake coefficients (i.e., reaction probabilities) of trace species onto atmospherically relevant surfaces. In other words, when determining reactive uptake coefficients of gas-phase species in the laboratory, one often needs to correct for concentration gradients in the experiments, which require accurate diffusion coefficients of the species under investigation.

Despite the importance of diffusion coefficients for predicting the heterogeneous loss of gas-phase species on atmospheric particles and cloud droplets and also for analyzing laboratory data, accurate values of this parameter in many cases do not

* Corresponding author. E-mail: avivanov@ucsd.edu.
† Permanent address: Center for Green Chemistry, University of Massachusetts-Lowell, Lowell, MA 01886.
‡ Permanent address: Department of Chemistry, University of British Columbia, Vancouver, BC, Canada V6T 1Z3.
§ Permanent address: Department of Kinetics and Catalysis, Semenov Institute of Chemical Physics, Russian Academy of Sciences, Moscow 117997, Russia.

10.1021/jp066558w CCC: $37.00
Published on Web 02/14/2007

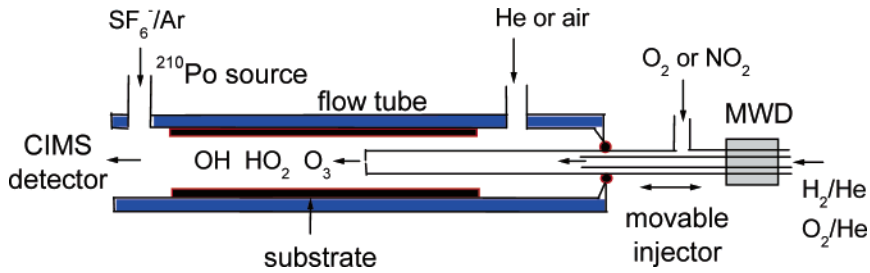

Figure 1. Schematic diagram of the fast flow-tube reactor coupled to CIMS.

exist. This is especially true for OH, HO_2, and O_3. In air or He, there has been only one measurement for HO_2[9], no measurements for O_3, and two measurements for OH.[1,12] Furthermore, in one of the two previous OH studies, there was a large uncertainty associated with the measurement. Clearly more work in this area is required.

In the following we measured the diffusion of OH, HO_2, and O_3 in He, and OH in air. Note that measurements in He are beneficial since most laboratory studies of reactive uptake coefficients use He as a carrier gas, and hence, these laboratory studies require the diffusion coefficient of OH in He to analyze their laboratory data. Also, measurements of diffusion coefficients in He can be used to test theoretical calculations.

In addition to measuring diffusion coefficients, we have compared the diffusion coefficients for OH and HO_2 with the measured diffusion coefficients of their nonpolar analogues (O and O_2) and the measured diffusion coefficients of the polar analogue (H_2O and H_2O_2). In the past, researchers have used the nonpolar analogues to estimate the diffusion coefficients of OH and HO_2. Our comparison shows that the diffusion coefficients of OH and HO_2 are closer to their polar analogues than the nonpolar analogues, and hence the nonpolar analogues should not be used for estimate the transport properties of OH and HO_2, rather the polar analogues should be used (or calculations based on the polar analogues) when no direct measurements of the diffusion coefficients of OH and HO_2 are available.

In addition we compared our results for OH, HO_2, and O_3 to calculations of the diffusion coefficients based on the Lennard-Jones potential. For OH and HO_2, we used the collision parameters of the polar analogues. We show the calculations are in excellent agreement with the measurements, and hence this model can be used to predict diffusion coefficients accurately for conditions where no laboratory data exist.

Experimental Section

To determine diffusion coefficients of HO_x and O_3, we measured the first-order loss rate of these species to reactive surfaces as a function of pressure using a coated-wall flow tube reactor. Then the pressure dependent data were analyzed using the rule of additivity of kinetic resistances to yield diffusion coefficients.

The first-order loss rates of HO_x and O_3 to various reactive surfaces as a function of pressure were determined using a coated-wall flow tube reactor coupled to a chemical ionization mass spectrometer (see Figure 1).[1,2,19] The flow tube, 2.5 cm i.d. by 25 cm long, was constructed of borosilicate glass and included a movable injector through which OH, HO_2, or O_3 was introduced. Helium or air, the main carrier gas, was introduced through a port at the upstream end of the flow reactor. All flow rates were determined with calibrated electronic mass flow meters (Tylan General) or by monitoring the rate of change of pressure in a known volume. Typical conditions in the flow tube were 12−40 m s^{-1} flow velocity of He or air at 1.0−6.3 Torr. A typical experiment consisted of measuring the OH, HO_2, or O_3 signal as a function of injector position. The signal was then plotted as a function of reaction time to determine the first-order loss rate coefficient, k_{obs}, at the flow tube wall. This whole process was then repeated at various pressures to obtain k_{obs} as a function of pressure.

A movable injector was used as a radical (OH, HO_2) or O_3 source. The following reactions were used to generate the species:

OH source 1: $H + NO_2 \rightarrow OH + NO$

OH source 2: $H_2O \rightarrow OH + H$

(a microwave discharge of H_2O vapor in He)

OH source 3: $H + O_2 + M \rightarrow HO_2 + M$

$H + HO_2 \rightarrow 2\ OH$

HO_2 source: $H + O_2 + M \rightarrow HO_2 + M$

O_3 source: $O + O_2 + M \rightarrow O_3 + M$

See references 1 and 2 for more details on the HO_x and O_3 sources. Typical HO_x and O_3 concentrations were less than 10^{10} molecule cm^{-3}. Under these conditions the gas-phase secondary chemistry was not important.

For the CIMS measurements, SF_6^- was used as the reagent ion for detection of O_3 and OH, and F^- was used as the reagent ion for detection of HO_2. The following equations describe the important chemistry:

$$OH + SF_6^- \rightarrow OH^- + SF_6$$

$$O_3 + SF_6^- \rightarrow O_3^- + SF_6$$

$$HO_2 + F^- \rightarrow O_2^- + HF$$

SF_6^- and F^- were produced by combining trace amounts of SF_6 and F_2, respectively, with Ar and then passing the mixture through a ^{210}Po ion source. The CIMS sensitivity was found to be $\sim 10^6$ molecules cm^{-3} for OH, $2 \cdot 10^6$ molecules cm^{-3} for HO_2, and $\sim 10^8$ molecules cm^{-3} for O_3 at S/N = 1 and an integration time of 1 s.

The following reactive surfaces were used when determining k_{obs} as a function of pressure: for OH, an Al_2O_3 surface ($\gamma_{OH} = 0.2$) and octadecyltrichlorosilane (OTS), ($\gamma_{OH} \sim 1$) were used. [The values in the brackets represent the reaction probability or reactive uptake coefficient of the trace gas-phase species on the reactive surface.][1,2] For HO_2, an Al_2O_3 surface ($\gamma_{HO_2} = 0.013$) and methane-soot ($\gamma_{HO_2} = 0.05$) surface was used. Finally, for O_3, a methane-soot surface ($\gamma_{O_3} = 0.033$) was used. The uptake coefficient of O_3 on methane soot in round brackets was determined in the present experiments, where all other

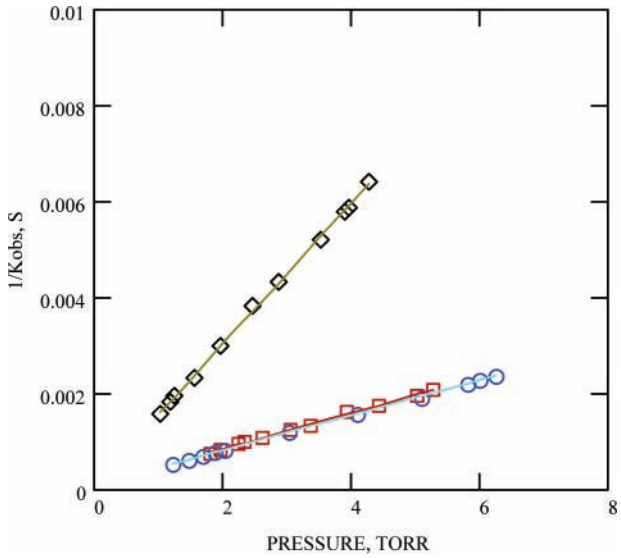

Figure 2. The pressure dependence of $1/k_{obs}$ of OH loss on Al_2O_3 (squares) and OTS (circles) in He and on Al_2O_3 (diamonds) in air. The solid lines are a linear least-squares fit to the data.

uptake coefficients were determined in previous measurements.[19] The methods of preparation of the surfaces are described in detail elsewhere.[1,2] In short, for the soot and OTS monolayer, a pyrex cylindrical tube was coated with the material and then inserted into the flow tube reactor. For the Al_2O_3 and graphite surfaces, a cylindrical tube constructed of Al_2O_3 and graphite, respectively, was inserted into the flow reactor.

The gases employed were He (BOC, 99.999%), synthetic air (BOC, grade 0.2), and NO_2 (Matheson, 99.5%). The surface materials used were Al_2O_3 (Aldrich, 99.9%), OTS (Aldrich, >90%), graphite (Aldrich, 99.9%), and methane soot produced from a methane-air flame.

As mentioned above, we determined the first-order loss rate (specifically the first-order loss rate coefficient, k_{obs}) of HO_x and O_3 on the reactive surfaces as a function of pressure. The data were then analyzed using the rule of additivity of kinetic resistances to determine diffusion coefficients. For a cylindrical reactor, the observed first-order loss rate coefficient at the flow tube wall, k_{obs}, can be described by the following equation:[20]

$$\frac{1}{k_{obs}} = \frac{2r}{\gamma c_{avg}} + \left(\frac{r^2}{3.66 D_p}\right)p \qquad (4)$$

where p is the pressure (Torr), r is the radius of the flow tube reactor (cm), and D_p is the diffusion coefficient (Torr cm^2 s^{-1}). According to eq 4, a plot of $1/k_{obs}$ versus pressure gives a straight line with the slope inversely proportional to the diffusion coefficient. Also, the reactive uptake coefficient can be determined from the intercept. In our analysis, $1/k_{obs}$ was plotted as a function of pressure, and the diffusion coefficient was determined from the slope. The diffusion coefficients determined with this method were independent of the reactive uptake coefficient.

Results and Discussion

Prior to measuring the diffusion coefficients of HO_x and O_3, we first measured the diffusion coefficient of atomic oxygen in He, as a validation of our apparatus and method of data analysis. The diffusion coefficient of O has been measured in the past by several others, and hence represents a good test for our apparatus and methodology. Shown in Figure 4 is the dependence of the first-order loss rate constant of O on a graphite surface using a He carrier gas. From the slope of this plot, the following diffusion coefficient was obtained: $D_{O-He} = 756 \pm 40$ Torr cm^2 s^{-1}. The experimental finding is quite consistent with literature values, which range from 731 to 815 Torr cm^2 s^{-1}.[21−23] Note, that we have not considered the data reported in reference 31 when determining this range due to the criticisms reported in reference 22.

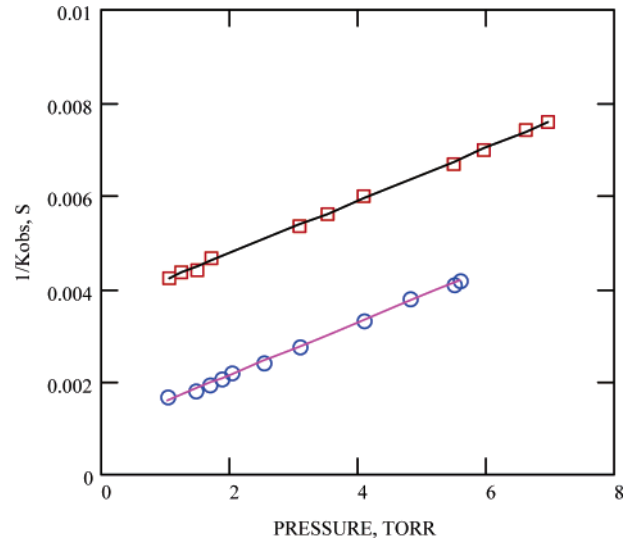

Figure 3. The pressure dependence of $1/k_{obs}$ of HO_2 loss on Al_2O_3 (squares) and soot (circles) in He. The solid lines are a linear least-squares fit to the data.

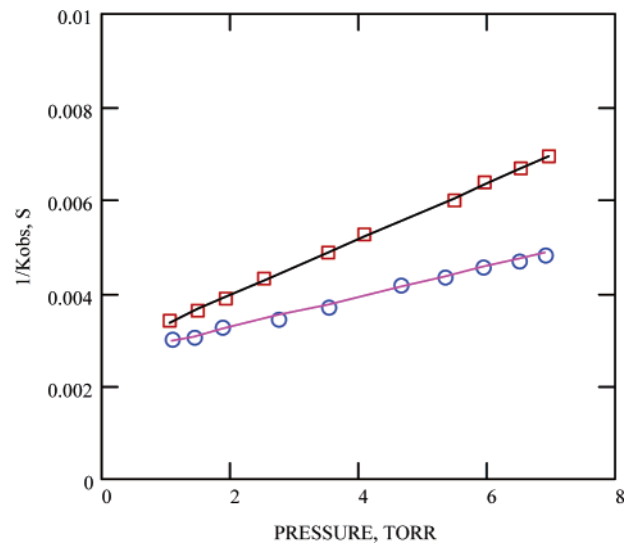

Figure 4. The pressure dependence of $1/k_{obs}$ of O_3 loss on soot (squares) and of O loss on graphite (circles) in He. The solid lines are a linear least-squares fit to the data.

Measurements of the Diffusion Coefficients of HO_x and O_3 and Comparison with Previous Measurements. Shown in Figure 2 is a plot of the typical pressure dependences of the observed first-order loss rate coefficient of OH on Al_2O_3 and OTS surfaces with He as a carrier gas. Both dependences reveal very close values of 657 ± 25 Torr cm^2 s^{-1} and 674 ± 25 Torr cm^2 s^{-1} using the inorganic and organic surfaces. Based on our measurements of the diffusion coefficient, the average value is $D_{OH-He} = 662 \pm 33$ Torr cm^2 s^{-1}. Figure 2 also shows the pressure dependence in synthetic air. The diffusion coefficient determined from this plot is $D_{OH-air} = 163 \pm 20$ Torr cm^2 s^{-1}. Figure 3 illustrates the similar pressure-dependent heterogeneous loss of HO_2 on Al_2O_3 and methane-soot surfaces. The measured

TABLE 1: Diffusion Coefficients of OH, HO_2 and O_3 at 1 Torr and 296 K

partner 1	partner 2	D_{12}, cm^2 s^{-1}	ref
OH ($X^2\Pi$)	He	662 ± 33	this study
		609 ± 250	24
		665 ± 35	1
	air	163 ± 20	this study
HO_2 (X^2A)	He	430 ± 30	this study
		405 ± 50	25
O_3 ($^1A_1$)	He	410 ± 25	this study

diffusion coefficients are $D_{HO_2-He} = 430 \pm 30$ Torr cm^2 s^{-1} for both surfaces. The dependences of O_3 loss on the methane-soot surface in He are shown in Figure 4. The value obtained is $D_{O_3-He} = 410 \pm 25$ Torr cm^2 s^{-1}.

The results from our measurements together with previous measurements of HO_x diffusion coefficients are summarized in Table 1.[1,24,25] The previous measurements also used the rule of additivity of kinetic resistances and flow tube reactors to determine diffusion coefficients.[1,9,26] The data summarized in Table 1 show that our measurements are consistent with previous measurements, and also highlight the fact that the measurements reported in this study significantly expand the available data on the diffusion coefficients of OH, HO_2 and O_3.

Surprisingly, to date there have been no direct measurements for the O_3 diffusion coefficient in He or air. An experimental assessment,[27] where the diffusion coefficient of O_3 in air was inferred from a complex system of reactions, produced an estimated value of 230 to 460 Torr cm^2 s^{-1} at room temperature. There are also two theoretical estimates[28,29] of the O_3 diffusion coefficient in O_2, which range from 91 to 205 Torr cm^2 s^{-1} at 298−300 K. Also, there is an estimate[30] of 394 Torr cm^2 s^{-1} for the O_3 diffusion coefficient in He at 298 K based on averaging the diffusion coefficients of stable molecules SO_2, CO_2, and NOCl, which is in reasonable agreement with our measured value. This latter value has been used in the past when analyzing laboratory measurements of reactive uptake coefficients.[30]

Comparison between Measured Diffusion Coefficients of HO_x and Measured Diffusion Coefficients of Polar and Nonpolar Analogues. In the past, researchers have used the diffusion coefficients of O and O_2 (nonpolar analogues for OH and HO_2, respectively) to approximate the diffusion coefficients of OH and HO_2.[6,13] In Table 2 we compare our measured diffusion coefficients of HO_x with the measured diffusion coefficients of the nonpolar analogues (O and O_2)[21−23,31−39] as well as measured diffusions coefficients of the polar analogues (H_2O and H_2O_2).[40−43] The measured diffusion coefficients for OH in He are in much better agreement with the polar analogue (H_2O) than the nonpolar analogue (O). The measured diffusion coefficient for OH in air also appears to follow a similar trend, although definitive conclusions are not possible due to the large uncertainty in the measured diffusion coefficients of H_2O in air. In addition, OH diffusion differs from that of O by 11% in He and by 25% in air. From the HO_2 data, we can also conclude that the measured diffusion coefficient of HO_2 in He is not in good agreement with the measured diffusion coefficient of the nonpolar analogue (O_2) in He: HO_2 diffusion is approximately 28% lower compared to O_2 in He. Based on this, we conclude that the nonpolar analogue should not be used for estimate the transport properties of OH and HO_2, rather the polar analogues should be used (or calculations based on the polar analogues; see below) when no direct measurements of the diffusion coefficients of OH and HO_2 are available. Note this conclusion has been made previously in the literature based on a limited data set.[1,9] Our results provide stronger support for this conclusion.

The trend observed in Table 2 can be rationalized with the dipole moments of the molecules or atoms. The dipole moments of OH and HO_2 are 1.74[44] and 2.090 ± 0.034,[45] respectively. The dipole moments of H_2O and H_2O_2 are 1.82[46] and 2.13 ± 0.05,[46] respectively, whereas the dipole moment of O and O_2 are both zero. A radical has a smaller diffusion coefficient than its nonpolar analogues since the radical diffusion is determined for the most part by the anisotropy of the atom−radical and molecule−radical interaction potentials, which is related to the dipole moments. For example, the anisotropy of interactions involving both OH and H_2O are certainly much larger than those of interactions involving O atoms, due to the dipole moments. This result also applies to HO_2 and H_2O_2 versus O_2. In addition, the presence of the body-fixed dipole moment in OH, H_2O, HO_2, and H_2O_2 makes the interactions involving these species much stronger. As a result, HO_x radical diffusion is expected to be slower in both nonpolar and polar gases.

Comparisons between the Measured Diffusion Coefficients and Calculations based on the 6−12 Lennard−Jones Potential Model. When calculating diffusion coefficients, we used the 6−12 Lennard−Jones potential model[47] to describe the interactions between gas-phase species:

$$\varphi(r) = 4\epsilon[(\sigma/r)^{12} - (\sigma/r)^6]$$

where $\varphi(r)$ is the 6−12 Lennard-Jones potential and r is the distance between two molecules. This model describes reasonably well the interaction between simple nonpolar molecules and includes the following two parameters: σ (the collision diameter at $\varphi(r) = 0$) and ϵ (the potential well depth where the attraction energy is maximum $r = 2^{1/6}\sigma$), which are constants characteristic of the colliding molecules.

In kinetic theory of dilute gases, a transport coefficient such as a diffusion coefficient is expressed in terms of a set of reduced collision integrals, which in turn depend on the potential model that describes the molecular interaction. Within the Lennard−

TABLE 2: Comparison between Our Measured Diffusion Coefficients of HO_x and Measured Diffusion Coefficients of the Nonpolar and Polar Analogues

partner 1	partner 2	measured (this study)	measured diffusion coefficient of the polar analogues	measured diffusion coefficient of the nonpolar analogue
OH	He	662 ± 33	646−690[a]	731−815[b]
	air	163 ± 20	154−241[c]	205−243[d]
HO_2	He	430 ± 30	ND	538−559[e]
	Air	ND	111−116[f]	158−175[g]

[a] Based on refs 40−42. [b] Based on refs 21−23, we have not considered the data reported in reference 31 when determining this range due to the criticisms reported in reference 22. [c] Based on refs 41−42. [d] Based on the diffusion in O_2 reported in refs 21, 31, 32 [note, the diffusion in O_2 is expected to be within a few percent of the diffusion in air]. [e] Based on refs 33−36. [f] Extrapolated from ref 43 using a $T^{1.92}$ dependence; the temperature dependence was determined by first calculating the diffusion coefficient of H_2O_2 in air for temperatures ranging from 20 to 5000 K and then by fitting the temperature-dependent data. [g] Based on the diffusion in N_2, reported in refs 32, 37−39; ND, not determined or data is not available.

Jones potential model, the ordinary diffusion coefficient is determined as follows:[47]

$$D(T) = \frac{0.002628T^{1.5}}{(2\mu)^{0.5}\sigma^2 <\Omega^{(1,1)*}(\theta)>}, \quad \text{atm cm}^2\ \text{s}^{-1} \qquad (5)$$

where T is temperature, μ is the reduced mass of the colliding species, $<\Omega^{(1,1)*}(\theta)>$ is the collision integral normalized to its rigid sphere value, $\theta = kT/\epsilon$ is the reduced temperature, and k is Boltzmann's constant. The normalized collision integrals are calculated analytically, and their values are normally tabulated (see, for example, ref 47).

The parameters σ and ϵ of the individual species are required when calculating diffusion coefficients. Normally these parameters are obtained by analysis of the experimental data for second virial coefficients, transport coefficients, and constants characteristic of the critical temperature, melting and boiling points, or by quantum mechanics calculations. These values are known for O_3 (see Table 3a), but there is no such data for OH and HO_2 radicals. In our calculations, we used the σ and ϵ parameters of H_2O to estimate the OH diffusion coefficient and the parameters of H_2O_2 for the HO_2 diffusion coefficient (see Table 3a for a complete list of the parameters for the individual species used in our calculations).[9,48,49]

Parameters used for calculations of binary diffusion coefficients can be approximated with the parameters of individual species within the Lennard-Jones potential model according to the combination rules:[41]

$$\sigma_{ij} = \frac{\sigma_i + \sigma_j}{2} \quad \epsilon_{ij} = (\epsilon_i \epsilon_j)^{0.5} \qquad (6)$$

Shown in Table 3b is the binary force constants calculated using eq 6. The binary diffusion coefficient describes the ordinary diffusion of a pair of species when only two species are present. However, it is also practical to describe the diffusion coefficient when other species are present.

An estimate of the binary diffusion coefficient in a mixture of several gases can be obtained based on Blanc's law:[50]

$$\frac{1}{D_{\text{mix}}} = \sum_i \frac{\chi_i}{D_i} \qquad (7)$$

where χ_i and D_i are the mole fraction and diffusion coefficient of each component of a mixture.

The results of the calculations are compared with the experimental measurements in Table 4. The calculations for OH, HO_2, and O_3 are in excellent agreement with our measured diffusion coefficients. This provides strong support that this model can be used to predict diffusion coefficients accurately for conditions where no laboratory data exist. For example, this model could be used with high confidence to predict the diffusion coefficient of O_3 in air or HO_2 in air, where measurements have not been performed. Also, the comparison in Table 4 provides stronger support that the diffusion coefficients of OH and HO_2 can be described with high confidence using the collision parameters for the polar analogues.

Our calculations above for OH and HO_2 are similar to the calculations used by Hanson et al. to estimate the diffusion coefficient of OH and HO_2 in a H_2O buffer gas. However, these authors used the diffusion coefficients of O and O_2 (the nonpolar analogues) rather than the polar analogues to represented the diffusion coefficients of OH and HO_2 in a He buffer gas. Our work (both Table 2 and Table 4) shows that a more accurate prediction of the diffusion coefficients will result if the polar analogues (H_2O and H_2O_2) are used when predicting the diffusion coefficients in a He buffer gas as well as a H_2O buffer gas. Further studies on the temperature dependence of radical diffusion are needed to verify if the polar analogue approximation is still valid at temperatures different from room temperature.

TABLE 3: Individual and Calculated Binary Force Constants

(a) Individual Force Constants

species	σ, Å	ϵ/k	ref
H_2O	2.641	809.1	49
H_2O_2	4.196	298.3	9
O_3	3.875	208.4	49
He	2.556	10.22	48
N_2	3.798	71.4	49
O_2	3.467	106.7	49

(b) Calculated Binary Force Constants

pairs	σ, Å	ϵ/k, K
H_2O-He	2.596	90.93
H_2O-N_2	3.220	240.35
H_2OO_2	3.054	293.82
H_2O-H_2O	2.641	809.1
H_2O_2-He	3.373	55.21
$H_2O_2-N_2$	3.997	145.94
$H_2O_2-O_2$	3.832	178.41
$H_2O_2-H_2O$	3.418	491.28
O_3-He	3.086	88.489
O_3-N_2	3.709	233.86
O_3-O_2	3.543	285.89
O_3-H_2O	3.131	787.26

TABLE 4: Comparison Our Experimental and Calculated (Based on the Polar Analogues for HO_x) Diffusion Coefficients of OH, HO_2, and O_3 at 1 Torr and 296 K[a]

		D_{12}, cm^2 s^{-1}	
partner 1	partner 2	measured	calculated
OH	He	662 ± 33	636.7
	air	163 ± 20	163.9
HO_2	He	430 ± 30	407.3
	air	ND	107.1
O_3	He	410 ± 25	425.4
	air	ND	96.3

[a] ND, not determined or data is not available.

Conclusions

In the present study, the diffusion coefficients of OH, HO_2 and O_3 in He and OH in air were experimentally measured. On the basis of the obtained results, we conclude that the diffusion of OH and HO_2 is closer to their dipole analogues, namely H_2O and H_2O_2, rather than to their non-dipole analogues O and O_2, respectively. The experimental results were also compared with theoretical predictions involving the (6−12) Lennard−Jones potential model. The calculations are in excellent agreement with the experimental measurements, which gives further confidence that these calculations can be used to estimate accurate diffusion coefficients for conditions where no data currently exists. Also the calculations show that diffusion coefficients of OH and HO_2 can be accurately represented using collision parameters of the polar analogues (H_2O and H_2O_2), giving further support that the diffusion of OH and HO_2 can be more accurately represented in the atmosphere by their dipole analogues.

Acknowledgment. This study was supported partially by NSF (ATM-003563) and NASA (NAG5-12707) grants. AKB

acknowledges funding support from NSERC. YMG acknowledges funding support from the Russian Foundation for Basic Research (RFBR 06-05-64602).

References and Notes

(1) Bertram, A. K.; Ivanov, A. V.; Hunter, M.; Molina, L. T.; Molina, M. J. *J. Phys. Chem. A* **2001**, *105*, 9415.
(2) Molina, M. J.; Ivanov, A. V.; Trakhtenberg, S.; Molina, L. T. *Geophys. Res. Lett.* **2004**, *31*, L22104.
(3) Chameides, W. L.; Davis, D. D. *J. Geophys. Res.* **1982**, *87*, 4863.
(4) Schwartz, S. E. *J. Geophys. Res.* **1984**, *89*, 1589.
(5) Schwartz S. E. in: W. Jaeschke (ed.), *Chemistry of Multiphase Atmospheric Systems*; Springer-Verlag: Berlin, 1986; p 415.
(6) Hanson, D. R.; Burkholder, J. B.; Howard, C. J.; Ravishankara, A. R. *J. Phys. Chem. A* **1992**, *96*, 4979.
(7) Takami, A.; Kato, S.; Shimono, A.; Koda, S. *Chem. Phys.* **1998**, *231*, 215.
(8) Mozurkewich, M.; McMurry, P. H.; Gupta, A.; Calvert, J. G. *J. Geophys. Res.* **1987**, *92*, 4163.
(9) Gershenzon, Y. M.; Grigorieva, V. M.; Ivanov, A. V.; Remorov, R. G. *Faraday Discuss.* **1995**, *100*, 83.
(10) Ivanov, A. V.; Gershenzon, Y. M.; Gratpanche, F.; Devolder, P.; Sawerysyn, J.-P. *Ann. Geophys.* **1996**, *14*, 659.
(11) Gershenzon, Y. M.; Grigorieva, V. M.; Zasypkin, A. Y.; Ivanov, A. V.; Remorov, R. G.; Aptekar, E. L. *Chem. Phys. Reports* **1999**, *18*, 79.
(12) Gershenzon, Y. M.; Ivanov, A. V.; Kucheryavyi, S. I.; Rozenshtein, V. B. *Kinet. Catalysis* **1986**, *27*, 923.
(13) Cooper, P. L.; Abbatt, J. P. D. *J. Phys. Chem.* **1996**, *100*, 2249.
(14) Ivanov, A. V.; Remorov, R. G.; Iliin, Y. S.; Gershenzon, M. Y.; Zasypkin, A. Y.; Gershenzon Y. M. In *Proc. Symp. EUROTRAC*, 2nd ed.; Borell, P. M., Borell, A., Eds.; WIT Press: Boston, 1998; Vol. 1, p 599.
(15) Meilinger, S. K.; Kärcher, B.; von Kuhlmann, R.; Peter, T. *Geophys. Res. Lett.* **2001**, *28*, 515.
(16) Jaegle, L.; Jacob, D. J.; Brune, W. H.; Faloona, I.; Tan, D.; Heikes, B. G.; Kondo, Y.; Sachse, G. W.; Anderson, B.; Gregory, G. L.; Singh, H. B.; Pueschel, R.; Ferry, G.; Blake, D. R.; Shetter, R. E. *J. Geophys. Res.* **2000**, *105*, 3877.
(17) Zuberi, B.; Johnson, K. S.; Aleks, G. K.; Molina, L. T.; Laskin, A. *Geophys. Res. Lett.* **2005**, *32*, L01807.
(18) Frank-Kamenetsky, D. A. *Diffusion and Heat Exchange in Chemical Kinetics*; Princeton University Press: Princeton, 1955.
(19) Ivanov, A. V.; Bertram, A. K.; Trakhtenberg, S.; Molina, L. T.; Molina, M. J. *5th Int. Conf. Chem. Kinetics*, July 16−20, 2001, Gaithersburg, MD; Book of Abstracts, 2001; p F37.
(20) Zasypkin, A. Y.; Grigorieva, V. M.; Korchak, V. N.; Gershenzon, Y. M. *Kinet. Catal.* **1997**, *38*, 772.
(21) Morgan, J. E.; Schiff, H. I. *Can. J. Chem.* **1964**, *42*, 2300.
(22) Judeikis, H. S.; Wun, M. *J. Chem. Phys.* **1978**, *68*, 4123.
(23) Plumb, I. C.; Ryan, K. R.; Barton, N. G. *Int. J. Chem. Kinet.* **1983**, *15*, 1081.
(24) Remorov, R. G.; Grigorieva, V. M.; Ivanov, A. V.; Sawerysyn, J.-P.; Gershenzon, Y. M. *13th Int. Symp. Gas Kinetics*, Dublin, Ireland, 11−16, 1996 Sept., Book of abstract, 417, 1996.
(25) Bedzhanian, Y.; Lelievre, S.; Le Bras, G. *Phys. Chem. Chem. Phys.* **2005**, *7*, 334.
(26) Ivanov, A. V.; Bertram, A. K.; Gershenzon, Y. M.; Molina, L. T.; Molina, M. J. *17th Int. Symp. Gas Kinetics*, Aug 24th-29th, Essen, Germany, Book of abstracts, XO.04, 2002.
(27) Hegeler, F.; Akiyama, H. *IEEE Transac. Plasma. Sci.* **1997**, *25*, 1158.
(28) Eliasson, B.; Hirth, M.; Kogelschatz, U. *J. Phys. D, App. Phys.* **1987**, *20*, 1421.
(29) Wen, J.; Thiemens, M. H. *J. Geophys. Res.* **1991**, *96*, 10911.
(30) Moise, T.; Rudich, Y. *J. Geophys. Res.*, **2000**, *105*, 14667.
(31) Yolles, R. S.; Wise, H. *J. Chem. Phys.* **1968**, *48*, 5109.
(32) Belyaev, Y. N.; Leonas, V. B. *High Temp. (USSR)* **1966**, *4*, 686.
(33) Giddings, J. C.; Seager, S. L. *Ind. Eng. Chem.* **1962**, *1*, 277.
(34) Seager, S. L.; Geertson, L. R.; Giddings, J. C. *J. Chem. Eng. Data* **1963**, *8*, 168.
(35) Wasik, S. P.; McCulloh, K. E. *J. Res. Matl. Bur. Stand. (US)* **1969**, *73A*, 207.
(36) Kestin, J.; Khalifa, H. E.; Ro, S. T.; Wakeham, W. A. *Physica* **1977**, *88A*, 242.
(37) Arnikar, H. J.; Rao, T. S.; Karmarkar, K. H. *Int. J. Electron.* **1967**, *22*, 381.
(38) Weissmann, S.; Mason, E. A. *J. Chem. Phys.* **1962**, *37*, 1289.
(39) Saxena, S. C.; Gupta, G. P. *J. Chem. Eng. Data* **1970**, *15*, 98.
(40) Schwertz, F. A.; Brow, J. E. *J. Chem. Phys.* **1951**, *19*, 640.
(41) Marrero, T. R.; Mason, E. A. *J. Phys. Chem. Ref. Data* **1972**, *1*, 3.
(42) Lee, C. Y.; Wilkie, C. R. *Ind. Eng. Chem.* **1954**, *46*, 2381.
(43) McMurtrie, R. L.; Keyes, F. G. *J. Am. Chem. Soc.* **1948**, *70*, 3755.
(44) Buldakov, M. A.; Cherepanov, V. N. *J. Phys. B* **2004**, *37*, 3973.
(45) Saito, S.; Matsumura, C. *J. Mol. Spec.* **1980**, *80*, 34.
(46) West, R. C. *CRC Handbook of Chemistry and Physics*, 65th ed.; CRC Press: Boca Raton, FL, 1984.
(47) Hirschfelder, J. O.; Curtis, C. F.; Bird, R. B. *Molecular Theory of Gases and Liquids*; John Wiley and Sons: New York, 1954. Reid, R. C.; Sherwood, T. K. *The Properties of Gases and Liquids*; McGraw-Hill: New York, 1958.
(48) Mason, E. A.; Monchick, L. *J. Chem. Phys.* **1962**, *36*, 2746.
(49) Massman, W. J. *Atm. Environ.* **1998**, *32*, 1111.
(50) Blanc, M. A. *J. Phys.* **1908**, *7*, 825.